Computational Assessment of the Effect of $\sigma-\pi$ Bonding Synergy and Reorganization Energies on Experimental Trends in Rhodium−Phosphine Bond Enthalpies

Clark R. Landis,* Steven Feldgus, Jamal Uddin, and Chris E. Wozniak

Department of Chemistry, University of Wisconsin, Madison, Wisconsin 53706

Kenneth G. Moloy

Central Research and Development Department, E. I. du Pont de Nemours & Co., Inc., Experimental Station, P.O. Box 80328, Wilmington, Delaware 19880-0328

Received June 23, 2000

Via a series of systematic density functional (B3LYP/LANL2DZ) computational experiments, we have examined the origin of opposing $Rh-PR_3$ bond enthalpy trends involving two different square-planar Rh(I) complexes with a series of different π-accepting phosphines (Huang, J. K.; Haar, C. M.; Nolan, S. P.; Marshall, W. J.; Moloy, K. G. *J. Am. Chem. Soc.* **1998**, *120*, 7806). Computational results rule out reorganization energies as the cause of the contradictory trends in thermodynamic analyses of metal−ligand bonding. Rather, calculations show that synergy of σ-donor and π-acceptor ligands linked to a metal is pivotal for interpreting the contradictory trends in Rh−P bond enthalpies. We conclude that metal−phosphine bond energies cannot be regarded as intrinsic, universal, or transferable.

1. Introduction

The use of organotransition-metal−phosphine complexes in homogeneous catalysis is widespread[1] and encompasses industrially important processes such as hydroformylation[2] and hydrogenation.[3] Manipulation of the wide range of available phosphine ligand (PR_3) basicities and steric bulk allows for fine-tuning of the metal reactivity and selectivity in organometallic chemistry and catalysis.[4−6]

Metal−ligand bond enthalpies are critical to a fundamental understanding of transition-metal-catalyzed reaction mechanisms and metal−ligand bonding. Because of their widespread catalytic utility, rhodium complexes make particularly compelling cases for metal−ligand bond enthalpy analyses. As demonstrated by Blake and co-workers,[7] oxidative addition to square-planar rhodium(I) systems is an enthalpically driven process. The thermodynamic stability of rhodium−phosphine complexes has also been studied.[8] Goldman and co-workers determined the bond dissociation enthalpies of $Rh-N_2$, $Rh-H_2$, Rh−olefin, and Rh−acetylene complexes.[9] The enthalpy behind the decarbonylation of aldehydes by a coordinatively unsaturated rhodium system was also determined by the same group. More recent results from Hartwig demonstrating C−H bond activation and functionalization with B−B reagents clearly illustrate the importance of understanding Rh−ligand bond enthalpies in devising new catalytic transformations.[10] A variety of methods have been used to study stereoelectronic contributions of the metal−ligand bond.[11−13] Solution calorimetric[18] techniques are popular for studying bond enthalpies in tertiary phosphine based systems such as organoruthe-

(1) (a) Collman, J. P.; Hegedus, L. S.; Norton, J. R.; Finke, R. G. *Principles and Applications of Organotransition Metal Chemistry*, 2nd ed.; University Science: Mill Valley, CA, 1987. (b) Parshall, G. W.; Ittel, S. D. *Homogeneous Catalysis*; Wiley-Interscience: New York, 1992.

(2) (a) Falbe, J. *Carbon Monoxide in Organic Synthesis*; Springer-Verlag: Berlin, 1980. (b) van Rooy, A.; de Bruijn, J. N. H.; Roobek, K. F.; Kamer, P. C. J.; Van Leeuwen, P. W. N. M. *J. Organomet. Chem.* **1996**, *507*, 69−73 and references cited therein.

(3) Noyori, R. *Asymmetric Catalysis in Organic Synthesis*; Wiley: New York, 1994, and references cited therein.

(4) (a) Hughes, R. P. In *Comprehensive Organometallic Chemistry*; Wilkinson, G., Stone, F. G. A., Abel, E. W., Eds.; Pergamon Press: Oxford, U.K., 1982; Chapter 35. (b) Sharp, P. R. In *Comprehensive Organometallic Chemistry II*; Wilkinson, G., Stone, F. G. A., Abel, E. W., Eds.; Pergamon Press: Oxford, U.K., 1995; Vol. 8, Chapter 2.

(5) (a) Tolman, C. A. *Chem. Rev.* **1977**, *77*, 313−348. (b) Manzer, L. E.; Tolman, C. A. *J. Am. Chem. Soc.* **1975**, *97*, 1955−1956.

(6) *Homogeneous Catalysis with Metal Phosphine Complexes*; Pignolet, L. H., Ed.; Plenum: New York, 1983.

(7) Mondal, J. U.; Blake, D. M. *Coord. Chem. Rev.* **1982**, *47*, 205−238 and references cited therein.

(8) Wang, K.; Goldman, A. S.; Li, C.; Nolan, S. P. *Organometallics* **1995**, *14*, 4010−4013.

(9) Wang, K.; Rosini, G. P.; Nolan, S. P.; Goldman, A. S. *J. Am. Chem. Soc.* **1995**, *117*, 5082−5088.

(10) Chen, H. Y.; Schlecht, S.; Semple, T. C.; Hartwig, J. F. *Science* **2000**, *287*, 1995−1997.

(11) (a) Rahman, M. M.; Liu, H.-Y.; Eriks, K.; Prock, A.; Giering, W. P. *Organometallics* **1989**, *8*, 1−7. (b) Liu, H.-Y.; Eriks, K.; Prock, A.; Giering, W. P. *Inorg. Chem.* **1989**, *28*, 1759−1763. (c) Poë, A. J. *Pure Appl. Chem.* **1988**, *60*, 1209−1216 and references cited therein. (d) Gao, Y.-C.; Shi, Q.-Z.; Kersher, D. L.; Basolo, F. *Inorg. Chem.* **1988**, *27*, 188−191. (e) Baker, R. T.; Calabrese, J. C.; Krusic, P. J.; Therien, M. J.; Trogler, W. C. *J. Am. Chem. Soc.* **1988**, *110*, 8392−8412. (f) Rahman, M. M.; Liu, H.-Y.; Prock, A.; Giering, W. P. *Organometallics* **1987**, *6*, 650−658.

(12) (a) Huynh, M. H. V.; Bessel, C. A.; Takeuchi, K. J. *Abstracts of Papers*, 208th Meeting of the American Chemical Society; American Chemical Society: Washington, DC, 1994; Abstract INOR 165. (b) Perez, W. J.; Bessel, C. A.; See, R. F.; Lake, C. H.; Churchill, M. R.; Takeuchi, K. J. *Abstracts of Papers*, 208th Meeting of the American Chemical Society; American Chemical Society: Washington, DC, 1994; INOR 166. (c) Ching, S.; Shriver, D. F. *J. Am. Chem. Soc.* **1989**, *111*, 3238−3243. (d) Lee, K.-W.; Brown, T. L. *Inorg. Chem.* **1987**, *26*, 1852−1856. (e) Brown, T. L.; Lee, K. J. *Coord. Chem. Rev.* **1993**, *128*, 89−116.

10.1021/om000544+ CCC: $19.00
Publication on Web 10/21/2000

nium,[14,19] organoiron,[15] organorhodium,[16,20,21] and organoplatinum[17] complexes. These techniques are also used to partition the steric and electronic effects of the phosphine ligands. For example, the enthalpies for reaction of Cp′Ru(COD)Cl (Cp′ = $-C_5H_5$, $-C_5Me_5$; COD = cyclooctadiene) with a series of *N*-pyrrolyl-substituted monodentate tertiary phosphine ligands to form Cp′Ru-$(PR_3)_2Cl$ (PR_3 = $P(NC_4H_4)_3$, $P(NC_4H_4)_2(C_6H_5)$, $P(NC_4H_4)(C_6H_5)_2$, $P(NC_4H_8)_3$)) have been measured and bond length−bond strength relationships determined. The Ru−P bond lengths decrease with increasingly π-withdrawing PR_3, while the reaction enthalpies (ΔH) increase.[19] In another system, Rh(acac)(CO)(PR_3), the reaction enthalpies decrease with the same ligands.[20]

Nolan, Moloy, et al. recently showed that the experimental enthalpies of reactions of square-planar rhodium(I) systems with different phosphines (reactions 1 and 2) having essentially the same steric bulk followed opposite trends.[21] Whereas the enthalpy of reaction 1

$$\text{RPNPRh(COE)} + PR_3 \rightarrow \text{RPNPRh}-PR_3 + \text{COE} \quad (1)$$

$$^1/_2[RhCl(CO)_2]_2 + 2PR_3 \rightarrow \textit{trans}\text{-RhCl(CO)}(PR_3)_2 + \text{CO} \quad (2)$$

becomes *less exothermic* with the addition of more basic phosphines, reaction 2 becomes *more exothermic*.[21] In the first reaction RPNP = $N(SiMe_2CH_2PPh_2)_2$, $N(SiMe_2CH_2P^iPr_2)_2$, COE = cyclooctene, and PR_3 is the series of *N*-pyrrolyl-substituted phosphine ligands $P(pyrl)_3$, $PPh(pyrl)_2$, $PPh_2(pyrl)$, and PPh_3 (pyrl = NC_4H_4, Ph = C_6H_5) (Chart 1).

Chart 1

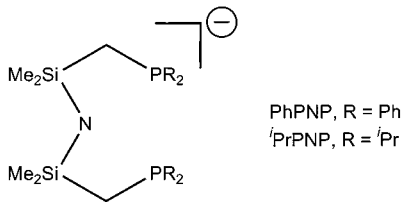

(a) bis(phosphino)-amido ligands RPNP

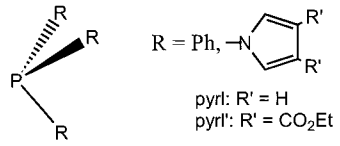

(b) tertiary phosphine ligands PR_3

The authors argued that reorganization energies, which are the amount of energy needed to deform the reacting fragments from their equilibrium geometry to the geometry in the complexes during the reaction, are responsible for the contradictory trends. It follows that in such cases the interpretation of a metal−ligand bond enthalpy as an intrinsic, universal, and transferable property (e.g., a "bond strength") is invalid. The rationalization by Nolan, Moloy, et al. of Rh−P bond enthalpy trends emphasizes three points: (1) the importance of reorganization energies of the phosphine system, (2) the importance of σ and π donor−acceptor interactions, and (3) the nontransferability of Rh−P bond strengths from one system to another.

In this paper we use DFT computations to explore Rh−P bond enthalpies in model systems closely related to the complexes examined by Nolan, Moloy, et al. The goals of this work are to establish the validity of DFT computations by comparison with experimental data and to explore the origins of the surprising trends revealed by the thermochemical measurements of Nolan, Moloy, et al.

2. Computational Details

To minimize computation time, we replaced cyclooctene with ethylene and the tridentate RPNP ligand was replaced by two different tridentate model ligands for reaction 1 (see Figure 1). The first is the model HPNP, where the bulky substituents on the silicon and phosphorus are replaced by hydrogens. The second is named FPNP, which is similar to HPNP, but hydrogens on phosphorus are replaced by fluorines. We used two different sets of PR_3 ligands. One series is PH_3, PH_2F, PHF_2, and PF_3, which have the Tolman electronic χ parameter[5] values of 24.9, 34.8, 44.7, and 54.6, respectively. Another series is PMe_3, PMe_2F, $PMeF_2$, and PF_3, which are better approximations to experimental ligands. The electronic χ parameter[5] values for PMe_3, PMe_2F, and $PMeF_2$ are 7.8, 23.4, and 39.0, respectively. The purpose of using fluorine instead of *N*-pyrrolyl in PR_3 is to speed computations while retaining the π-withdrawing character of the pyrrolyl substituents. For the PH_xF_{3-x} series small anomalies are observed in some of the computed trends, suggesting that H does not adequately simulate a phenyl group. These anomalies are removed when

(13) Lorsbach, B. A.; Prock, A.; Giering, W. P. *Organometallics* **1995**, *14*, 1694−1699 and references cited therein.

(14) For organoruthenium systems see: (a) Smith, D. C., Jr.; Haar, C. M.; Luo, L.; Li, C.; Cucullu, M. E.; Malher, C. H.; Nolan, S. P.; Marshall, W. J.; Jones, N. L.; Fagan, P. J. *Organometallics* **1999**, *18*, 2357−2361. (b) Serron, S. A.; Nolan, S. P. *Organometallics* **1995**, *14*, 4611−4616. (c) Luo, L.; Li, C.; Cucullu, M. E.; Nolan, S. P. *Organometallics* **1995**, *14*, 1333−1338. (d) Cucullu, M. E.; Luo, L.; Nolan, S. P.; Fagan, P. J.; Jones, N. L.; Calabrese, J. C. *Organometallics* **1995**, *14*, 289−296. (e) Luo, L.; Zhu, N.; Zhu, N. J.; Stevens, E. D.; Nolan, S. P.; Fagan, P. J. *Organometallics* **1994**, *13*, 669−675. (f) Li, C.; Cucullu, M. E.; McIntyre, R. A.; Stevens, E. D.; Nolan, S. P. *Organometallics* **1994**, *13*, 3621−3627. (g) Luo, L.; Nolan, S. P. *Organometallics* **1994**, *13*, 4781−4786. (h) Luo, L.; Fagan, P. J.; Nolan, S. P. *Organometallics* **1993**, *12*, 4305−4311.

(15) For organoiron systems see: (a) Li, C.; Stevens, E. D.; Nolan, S. P. *Organometallics* **1995**, *14*, 3791−3797. (b) Li, C.; Nolan, S. P. *Organometallics* **1995**, *14*, 1327−1331. (c) Luo, L.; Nolan, S. P. *Inorg. Chem.* **1993**, *32*, 2410−2415. (d) Luo, L.; Nolan, S. P. *Organometallics* **1992**, *11*, 3947−3951.

(16) For organorhodium systems see: (a) Haar, C. M.; Huang, J.; Nolan, S. P. *Organometallics* **1998**, *17*, 5018−5024. (b) Serron, S.; Nolan, S. P.; Moloy, K. G. *Organometallics* **1996**, *15*, 534−539.

(17) (a) Haar, C. M.; Nolan, S. N.; Marshall, W. J.; Moloy, K. G.; Prock, A.; Giering, W. P. *Organometallics* **1999**, *18*, 474−479. (b) Smith, D. C., Jr.; Haar, C. M.; Stevens, E. D.; Nolan, S. P.; Marshall, W. J.; Moloy, K. G. *Organometallics* **2000**, *19*, 1427−1433.

(18) Leading references include: (a) Nolan, S. P. Bonding Energetics of Organometallic Compounds. In *Encyclopedia of Inorganic Chemistry*; Wiley: New York, 1994. (b) Hoff, C. D. *Prog. Inorg. Chem.* **1992**, *40*, 503−561. (c) Martinho Simões, J. A.; Beauchamp, J. L. *Chem. Rev.* **1990**, *90*, 629−688. (d) *Bonding Energetics In Organometallic Compounds*; Marks, T. J., Ed.; ACS Symposium Series 428; American Chemical Society: Washington, DC, 1990. (e) Metal−Ligand Bonding Energetics in Organotransition Metal Compounds. *Polyhedron* **1988**, *7*. (f) Skinner, H. A.; Connor, J. A. In *Molecular Structure and Energetics*; Liebman, J. F., Greenberg, A., Eds.; VCH: New York, 1987; Vol. 2, Chapter 6.

(19) (a) Li, C.; Serron, S.; Nolan, S. P. *Organometallics* **1996**, *15*, 4020−4029. (b) Serron, S. A.; Luo, L.; Li, C.; Cucullu, M. E.; Nolan, S. P. *Organometallics* **1995**, *14*, 5290−5297.

(20) Sarron, S.; Huang, J.; Nolan. S. P. *Organometallics* **1998**, *17*, 534−539.

(21) Huang, J.; Haar, C. M.; Nolan, S. P.; Marshall, W. J.; Moloy, K. G. *J. Am. Chem. Soc.* **1998**, *120*, 7806−7815.

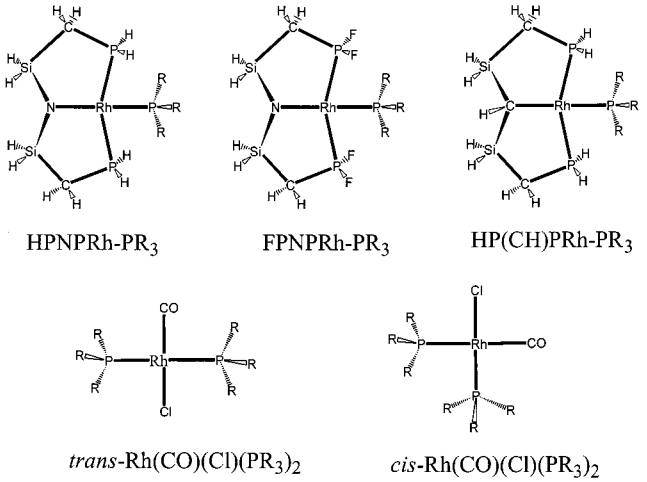

Figure 1. Model rhodium complexes used in the computations with R = H, Me, F.

we use the more realistic −Me group to model the phenyl group. The FPNPRh ligand model was devised to test the effect of adding a π-withdrawing substituent on the reaction 1 enthalpies. Bond energy decomposition analyses and charge decomposition analyses have been performed only with hydrogen- and fluorine-substituted phosphine complexes.

Two sets of geometry optimizations were performed using density functional theory (DFT) for the model systems. The first sets of geometry optimization and frequency calculation were done using Gaussian98[22a] and Gaussian94[22b] programs with Becke's three-parameter functional (B3)[23] and Lee, Yang, and Parr's (LYP)[24] correlation (B3LYP) with LANL2DZ basis sets which include Hay and Wadt's[25] double-ζ-quality basis set for the valence and penultimate shells, with effective core potentials at rhodium, Los Alamos ECP plus double-ζ on Si, S, and Cl,[26] and a Dunning−Huzinaga full double-ζ basis on C, H, N, and O.[27] The second set of optimizations were performed using the Amsterdam density functional (ADF) program developed by Baerends et al.[28] The basis set is of triple-ζ quality, augmented with two sets of polarization functions: 3d and 4f on S and 2p and 3d on H. The 1s2s2p core shells of S were treated by the frozen-core approximation.[28a,b] The MOs were expanded in a large uncontracted set of Slater type orbitals (STOs) containing diffuse functions TZP (no Gaussian basis functions are involved).[28c] All calculations were performed at the NL-SCF level, using the local density approximation (LDA), where exchange is described by Slater's

Scheme 1

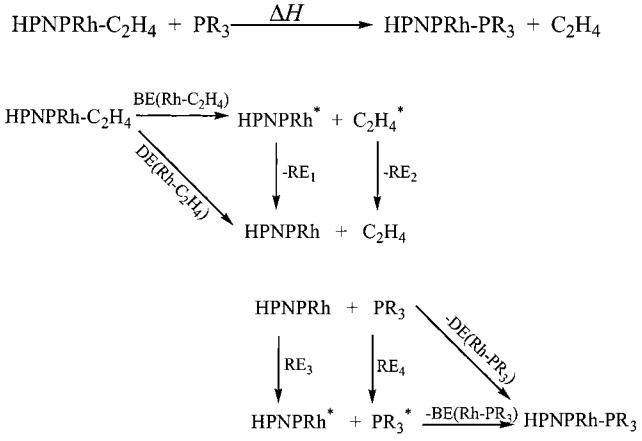

$$\Delta H = \mathrm{DE(Rh\text{-}C_2H_4)} - \mathrm{DE(Rh\text{-}PR_3)}$$

X potential[29] and the correlation is treated in the Vosko−Wilk−Nusair (VWN) parametrization,[28d] with nonlocal corrections for exchange (Becke88)[28e,f] and correlation due to Perdew[28g] added self-consistently[28h] (BP86).

A thermochemical cycle for reaction 1 (Scheme 1) illustrates the definitions of the reaction enthalpies ΔH, bond energies BE(M−L), dissociation energies DE(M−L), and reorganization energies RE(M−L). Reaction enthalpies were estimated by taking the differences in total energies between fully relaxed products and reactants for all bond-breaking and bond-forming steps.

Dissociation energies (e.g., DE(Rh−P)), alternatively called relaxed bond energies, express the difference in total energies between the fully relaxed metal−ligand complex (e.g., HPNPRh−PR_3) and the fully relaxed, dissociated fragments (HPNPRh and PR_3). Bond energies (BE) express the difference in total energies between the fully relaxed metal−ligand complex and the dissociated fragments (rigid) which are held at the geometries (other than metal−ligand bond length) of the metal−ligand complex. Fragments marked with an asterisk indicate that they have unrelaxed rigid geometry as in the complex. Reorganization energies (RE) equal the difference between the rigid (BE) and relaxed bond (DE) enthalpies. RE, BE, and DE are all intrinsically positive numbers as used herein. The net BEs plus the net REs for all species, as in Scheme 1, give the total reaction enthalpy, ΔH

$$\Delta H = \sum \mathrm{BE(M\text{-}L)} + \sum \mathrm{RE(M\text{-}L)}$$

$$\mathrm{DE(Rh\text{-}P)} = \mathrm{BE(Rh\text{-}P)} - \mathrm{RE(Rh\text{-}P)}$$

where $\sum$BE = BE(Rh−C_2H_4) − BE(Rh−PR_3) and $\sum$RE = (RE3 + RE4) − (RE1 + RE2) for reaction 1, as in Scheme 1.

Inspection of the bonding in the various systems was analyzed using natural bond orbital (NBO)[30] analysis and

(22) (a) Frisch, M. J.; Trucks, G. W.; Schlegel, H. B.; Scuseria, G. E.; Robb, M. A.; Cheeseman, J. R.; Zakrzewski, V. G.; Montgomery, J. A., Jr.; Stratmann, R. E.; Burant, J. C.; Dapprich, S.; Millam, J. M.; Daniels, A. D.; Kudin, K. N.; Strain, M. C.; Farkas, O.; Tomasi, J.; Barone, V.; Cossi, M.; Cammi, R.; Mennucci, B.; Pomelli, C.; Adamo, C.; Clifford, S.; Ochterski, J.; Petersson, G. A.; Ayala, P. Y.; Cui, Q.; Morokuma, K.; Malick, D. K.; Rabuck, A. D.; Raghavachari, K.; Foresman, J. B.; Cioslowski, J.; Ortiz, J. V.; Stefanov, B. B.; Liu, G.; Liashenko, A.; Piskorz, P.; Komaromi, I.; Gomperts, R.; Martin, R. L.; Fox, D. J.; Keith, T.; Al-Laham, M. A.; Peng, C. Y.; Nanayakkara, A.; Gonzalez, C.; Challacombe, M.; Gill, P. M. W.; Johnson, B. G.; Chen, W.; Wong, M. W.; Andres, J. L.; Head-Gordon, M.; Replogle, E. S.; Pople, J. A. *Gaussian 98*, revision A.7; Gaussian, Inc.: Pittsburgh, PA, 1998. (b) Frisch, M. J.; Trucks, G. W.; Schlegel, H. B.; Gill, P. M. W.; Johnson, B. G.; Robb, M. A.; Cheeseman, J. R.; Keith, T.; Petersson, G. A.; Montgomery, J. A.; Raghavachari, K.; Al-Laham, M. A.; Zakrzewski, V. G.; Ortiz, J. V.; Foresman, J. B.; Cioslowski, J.; Stefanov, B. B.; Nanayakkara, A.; Challacombe, M.; Peng, C. Y.; Ayala, P. Y.; Chen, W.; Wong, M. W.; Andres, J. L.; Replogle, E. S.; Gomperts, R.; Martin, R. L.; Fox, D. J.; Binkley, J. S.; Defrees, D. J.; Baker, J.; Stewart, J. P.; Head-Gordon, M.; Gonzalez, C.; Pople, J. A. *Gaussian 94*, revision D.4; Gaussian, Inc.: Pittsburgh, PA, 1995.
(23) Becke, A. D. *Phys. Rev. A* **1988**, *38*, 3098.
(24) Lee, C.; Yang, W.; Parr, R. G. *Phys. Rev. B* **1988**, *37*, 785−789.
(25) Hay, P. J.; Wadt, W. R. *J. Chem. Phys.* **1985**, *82*, 299−310.
(26) (a) Hay, P. J.; Wadt, W. R. *J. Chem. Phys.* **1985**, *82*, 270. (b) Hay, P. J.; Wadt, W. R. *J. Chem. Phys.* **1985**, *82*, 284.
(27) Dunning, T. H.; Hay, P. J. In *Modern Theoretical Chemistry*; Schaefer, H. F., III, Ed.; Plenum: New York, 1976; Vol. 3, p 1.
(28) (a) Fonseca Guerra, C.; Visser, O.; Snijders, J. G.; te Velde, G.; Baerends, E. J. In *Methods and Techniques for Computational Chemistry*; Clementi, E., Corongiu, G., Eds.; STEF: Cagliari, Italy, 1995; pp 305−395, and references therein. (b) Baerends, E. J.; Ellis, D. E.; Ros, P. *Chem. Phys.* **1973**, *2*, 41. (c) Snijders, J. G.; Baerends, E. J.; Vernooijs, P. *At. Nucl. Data Tables* **1982**, *26*, 483. (d) Vosko, S. H.; Wilk, L.; Nusair, M. *Can. J. Phys.* **1980**, *58*, 1200. (e) Becke, A. D. *J. Chem. Phys.* **1986**, *84*, 4524. (f) Becke, A. D. *Phys. Rev. A* **1988**, *38*, 3098. (g) Perdew, J. P. *Phys. Rev. B* **1986**, *33*, 8822; **1986**, *34*, 7406 (erratum). (h) Fan, L.; Ziegler, T. *J. Chem. Phys.* **1991**, *94*, 6057.
(29) Slater, J. C. *Quantum Theory of Molecules and Solids*; McGraw-Hill: New York, 1974; Vol. 4.
(30) Reed, A. E.; Curtiss, L. A.; Weinhold, F. *Chem. Rev.* **1988**, *88*, 899.

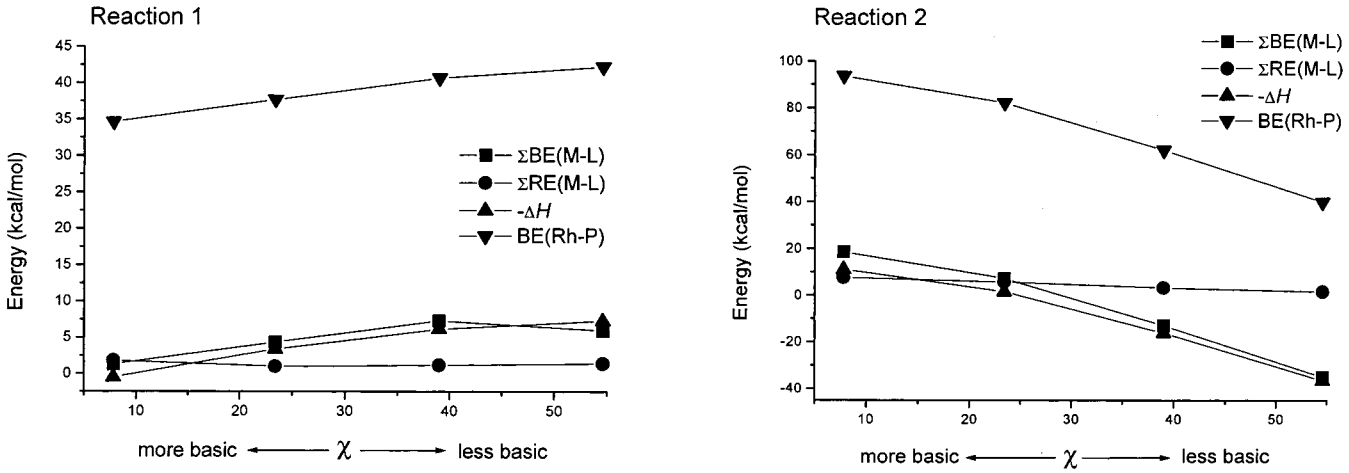

Figure 2. Calculated reaction enthalpies (ΔH), sum of rhodium−ligand bond energies $\sum$BE(M−L), and sum of reorganization energies $\sum$RE(M−L) for reaction 1 (left) and reaction 2 (right) plotted against Tolman χ parameters for the ligands PR_3 at the B3LYP/LANL2DZ level. The rhodium−phosphine bond dissociation energies BE(Rh−P) in HPNPRh−PR_3 and Rh(CO)(Cl)$(PR_3)_2$ complexes are also shown.

charge decomposition analysis (CDA).[31] These were performed using the same methods as in the Gaussian calculations. In the CDA method the molecular orbitals of the complex are expressed in terms of the MOs of appropriately chosen fragments. The CDA can be seen as a quantitative expression of the Dewar−Chatt−Duncanson (DCD) model[32] of synergistic metal−ligand bonding, which considers the ligand metal σ-donation and ligand metal π-back-donation as the dominant factors for the metal−ligand bond. The CDA calculations have been performed using the program CDA94.[33]

3. Results

(A) Computed Enthalpies of Reaction (ΔH) and Bond Energies (BE). The computational data for reactions 1 and 2, for the ligands PF_xMe_{3-x}, are shown in Figure 2, which demonstrates the computational reproduction of opposing trends for enthalpies of reactions 1 and 2 as a function of the Tolman electronic parameter. For reaction 1, the computed enthalpies for displacement of ethylene by a phosphine are significantly less exothermic than the experimental enthalpies for displacement of cyclooctene by phosphines in the solution, by approximately 25 kcal/mol for any given Tolman parameter of the phosphine ligand (Figure 3a). It is expected that cyclooctene binds more weakly than ethylene; hence, the experimental data should be more exothermic than our computed values. Most importantly, when the offset between computed and observed values is taken into account, the trends in the computed and observed reaction enthalpies for reaction 1 agree.

For reaction 2 the experimental and computed enthalpy trends agree, but there is a larger and less systematic offset. Solvation effects should be important because the reaction involves transformation of a relatively nonpolar dimer, $(RhCl(CO)_2)_2$, into the polar monomer $RhCl(CO)(PR_3)_2$. Because the experimental data are collected in a polar solvent (CH_2Cl_2) and our computations are for the gas phase, it is reasonable to expect that the experimental data will be considerably more exothermic than the gas-phase computation. When a constant offset between experiment and computation is taken into account, it is clear that our computations predict both the trend and range of bond energies observed empirically.

Is reorganization energy (RE) responsible for the opposing trends, both observed and computed, for reactions 1 and 2? As Figure 2 clearly depicts, reorganization energies are small and relatively constant for both reactions as the electronic parameter of the ligand is varied. Little geometric distortion of the ligand and metal fragment occurs upon coordination, and this distortion does not vary with the Tolman parameter of the phosphine. *Thus, the contradictory trends in reaction enthalpies are not due to reorganization energies*. Instead, we find the origin of the contradictory trends lies in variations of the Rh−P bond energies.

Table 1 shows calculated reaction enthalpies ΔH, the net bond energies $\sum$BE, and the net reorganization energies $\sum$RE along with the individual Rh−P bond energies BE(Rh−P) for reactions 1 and 2 for the model complexes. As the data in Table 1 and Figure 2 clearly demonstrate, computed and experimental reaction enthalpies strongly correlate with the individual Rh−P bond energies (BE(Rh−P)). Thus, the origin of the opposing trends in enthalpies for reactions 1 and 2 lies in the factors that determine the rhodium−phosphine bond energies BE(Rh−P).

Why does the Rh−P bond energy for HPNPRh−PR_3 decrease with increasing phosphine donor ability, whereas the Rh−P bond energy of Rh(CO)(Cl)$(PR_3)_2$ increases? We have examined several possible explanations: (1) the opposing trends are a manifestation of different trans influences in Rh(CO)(Cl)$(PR_3)_2$ and HPNPRhPR_3, (2) the Rh−P bond energy of complexes having at least one strong π-acid ligand, such as CO, increases with increasing donor ability due to synergistic donation-from-phosphine/back-donation-to-CO effects, and (3) the Rh center of Rh(CO)(Cl)$(PR_3)_2$ has a more positive effective charge than that of HPNPRh−PR_3.

(31) Dapprich, S.; Frenking, G. *J. Phys. Chem.* **1995**, *99*, 9352−9362.
(32) (a) Dewar, J. M. S. *Bull. Soc. Chim. Fr.* **1951**, *18*, 79. (b) Chatt, J.; Duncanson, L. A. *J. Chem. Soc.* **1953**, 2939.
(33) The CDA calculations were carried out with the program CDA 2.1: Dapprich, S.; Frenking, G. Phillips-Universität Marburg, 1994. The program is freely available: ftp.chemie.uni-marburg.de/pub/cda.

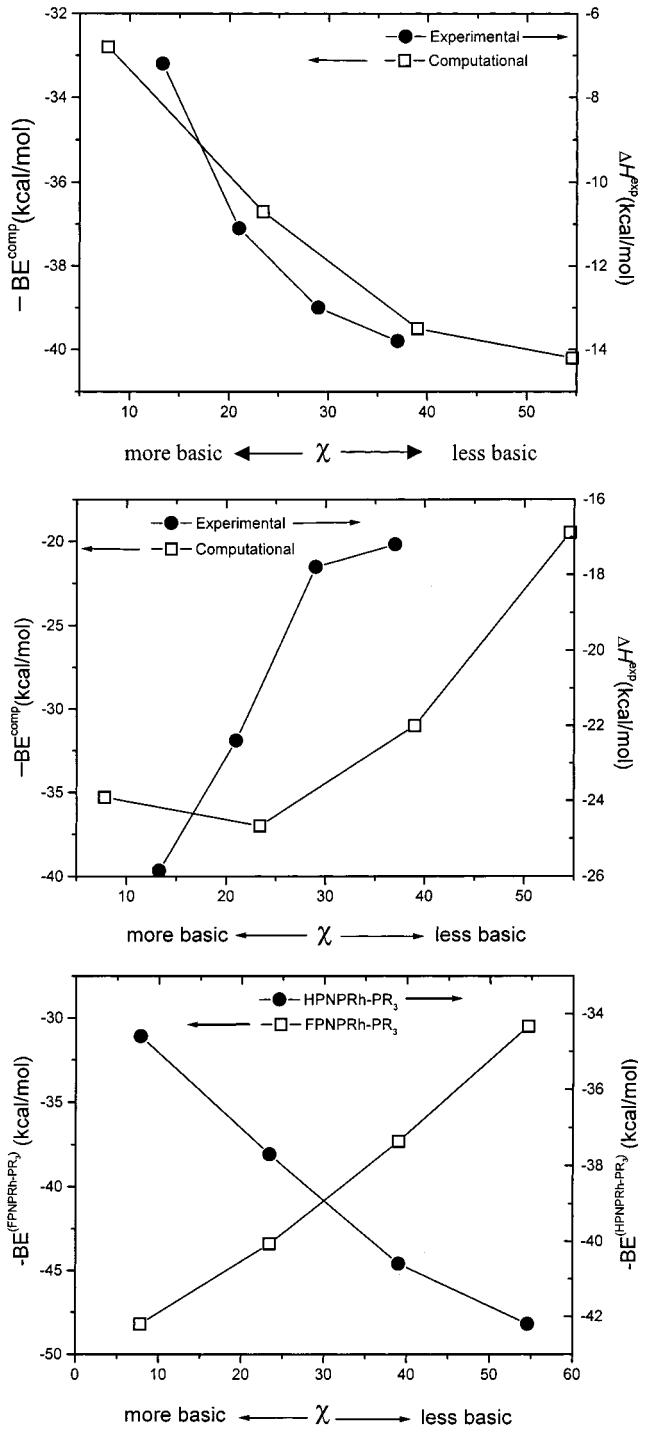

Figure 3. Calculated (B3LYP/LANL2DZ) bond energies BE(Rh−P): (a, top) in HPNPRh−PR_3 and experimental reaction enthalpies (ΔH) for reaction 1; (b, middle) in Rh(CO)(Cl)$(PR_3)_2$ and experimental reaction enthalpies (ΔH) for reaction 2. (c, bottom) Bond energies BE(Rh−P) calculated at the B3LYP/LANL2DZ level for model complexes HPNPRh−PR_3 and FPNPRh−PR_3 plotted against Tolman χ parameters for the ligands PR_3.

We conducted a series of computational experiments to distinguish among these effects. The model complexes, FPNPRh−PR_3 and HP(CH)PRh−PR_3, were devised as analogues of HPNPRh−PR_3 that contained strong π-acid capabilities and lacked π-donor abilities, respectively. Table 2 shows the Rh−PR_3 energy components of HPNPRh−PR_3, FPNPRh−PR_3, and HP(CH)PRh−PR_3 complexes computed at B3LYP/LANL2DZ. For HPNPRh−PR_3 the bond energies are shown for PR_xF_{3-x} with R = Me, H, whereas for FPNPRh−PR_3 only the R = Me results are shown. The reorganization energies are very small and do not reduce the interaction energy significantly in any of the complexes. The data in Table 2a and Figure 3a,c strikingly demonstrate *that making the HPNP ligand a strong π-acid (FPNP) by replacing the four P−H bonds with four P−F bonds reverses the trend of Rh−P bond energies as a function of Tolman χ parameter!* In contrast, we find that eliminating the π-donor capability of the amido N of the HPNP ligand by replacing it with −CH (HP(CH)P) decreases the absolute Rh−P bond energies by 7−10 kcal/mol but yields the same trend of decreasing Rh−P bond energies with increasing phosphine donor ability. These results are consistent with the expected stronger trans influence of C vs N, affecting the absolute Rh−P bond energies but not affecting their trends with respect to phosphine donor ability.

Table 1. Reaction Enthalpies (ΔH, in kcal/mol) for HPNPRh−C_2H_4 + PR_3 → HPNPRh−PR_3 + C_2H_4 (Reaction 1) and $^1/_2[RhCl(CO)_2]_2$ + 2PR_3 → *trans*-RhCl(CO)$(PR_3)_2$ + CO (Reaction 2) at the B3LYP/LANL2DZ Level of Theory

	PMe_3	PMe_2F	$PMeF_2$	PF_3
		Reaction 1		
ΣBE	1.28	4.32	7.29	5.90
ΣRE	1.81	0.97	1.15	1.37
ΔH	0.53	−3.35	−6.14	−7.27
BE(Rh−P)	34.60	37.65	40.63	42.20
		Reaction 2		
ΣBE	18.60	7.22	−12.97	−35.07
ΣRE	7.56	5.69	3.21	1.54
ΔH	−11.04	−1.52	16.18	36.62
BE(Rh−P)	93.55	82.20	61.99	39.92

Table 2. Bond Enthalpies (kcal/mol) According to the B3LYP/LANL2DZ Level of Theory

	PMe_3	PH_3	PMe_2F	PH_2F	$PMeF_2$	PHF_2	PF_3
(a) HPNPRh−PR_3, FPNPRh−PR_3 and HP(CH)PRh−PR_3							
			HPNPRh−PR_3				
BE(Rh−P)	34.61	30.50	37.65	39.44	40.63	43.01	42.20
RE(Rh−P)	1.82	3.16	0.97	3.25	1.14	1.75	2.02
DE(Rh−P)	32.79	27.34	36.68	36.19	39.49	41.26	40.18
			FPNPRh−PR_3				
BE(Rh−P)	48.23		43.39		37.33		30.54
			HP(CH)PRh−PR_3				
BE(Rh−P)		23.46		31.13		36.40	37.31
RE(Rh−P)		1.81		2.66		2.98	2.78
DE(Rh−P)	24.96	21.65	28.83	28.47	32.05	33.42	34.53
(b) Rh(CO)(Cl)$(PR_3)_2$							
			trans-Rh(CO)(Cl)PR_3−PR_3				
BE(Rh−P)	40.64	33.93	40.19	36.62	33.04	26.73	20.30
RE(Rh−P)	5.39	2.53	3.91	2.76	2.01	3.54	0.86
DE(Rh−P)	35.25	31.40	37.00	33.86	31.03	23.19	19.45
			cis-Rh(CO)(Cl)PR_3−PR_3[b]				
BE(Rh−P)	34.26		39.23		28.98		15.82
RE(Rh−P)	3.30		2.91		3.05		3.11
DE(Rh−P)	30.96		36.32		25.93		12.71

[a] BE(Rh−P) is the bond enthalpy for the unrelaxed fragments, RE is the enthalpy change in the fragments due to relaxation from rigid fragments, and DE(Rh−P) is the bond enthalpy for completely relaxed bond dissociation. [b] Calculations are shown for PR_3 trans to Cl. Reorganization energies of the fragments in the case of PR_3 trans to CO differ by less than 0.5 kcal/mol.

Table 3. Optimized Bond Lengths (Å) at B3LYP/LANL2DZ and BP86/TZ(P) Levels of Theory

	PMe_3	PH_3	PMe_2F	PH_2F	$PMeF_2$	PHF_2	PF_3
(a) HPNPRh−PR_3 and HP(CH)PRh−PR_3							
HPNPRh−PR_3							
Rh−P	2.368	2.353	2.302	2.284	2.259	2.247	2.232
	2.212[a]	2.216[b]		2.176[b]		2.145[b]	2.140,[a] 2.136[b]
Rh−N	2.121	2.125	2.102	2.104	2.083	2.077	2.065
	2.151[a]	2.136[b]		2.124[b]		2.110[b]	2.130,[a] 2.100[b]
Rh−P(1)	2.384	2.377	2.396	2.391	2.397	2.398	2.409
	2.292[a]	2.284[b]		2.297[b]		2.305[b]	2.326,[a] 2.307[b]
Rh−P(2)	2.377	2.377	2.392	2.382	2.389	2.389	2.392
	2.277[a]	2.284[b]		2.287[b]		2.295[b]	2.292,[a] 2.303[b]
FPNPRh−PR_3							
Rh−P	2.392		2.348		2.305		2.284
Rh−N	2.123		2.103		2.086		2.068
Rh−P(1)	2.312		2.318		2.318		2.342
Rh−P(2)	2.312		2.333		2.340		2.342
HP(CH)PRh−PR_3							
Rh−P	2.405	2.398	2.331	2.331	2.290	2.276	2.258
Rh−C	2.207	2.187	2.197	2.187	2.189	2.183	2.168
Rh−P(1)	2.377	2.380	2.384	2.377	2.383	2.386	2.393
Rh−P(2)	2.365	2.379	2.377	2.384	2.393	2.391	2.403
(b) Rh(CO)(Cl)$(PR_3)_3$							
Rh−P	2.412	2.393	2.380	2.354	2.359	2.350	2.348
		2.298[b]		2.268[b]		2.254[b]	2.251[b]
Rh−Cl	2.471	2.447	2.451	2.455	2.413	2.410	2.401
		2.377[b]		2.383[b]		2.356[b]	2.347[b]
Rh−C	1.829	1.842	1.849	1.858	1.868	1.873	1.892
		1.832[b]		1.844[b]		1.851[b]	1.861[b]
C−O	1.191	1.186	1.183	1.177	1.178	1.176	1.170
		1.166[b]		1.160[b]		1.160[b]	1.156[b]

[a] Experimental values: compared with PhPNPRh−$P(Ph)_3$ and PhPNPRh−$P(pyrl)_3$ experimental geometries. [b] BP86/TZ(P).

Next we consider the possibility that trans influences in Rh(CO)(Cl)$(PR_3)_2$ dominate the observed enthalpy trends. In Table 2b, the contributing terms of bond energies for Rh−PR_3 in *trans*-Rh(CO)(Cl)$(PR_3)_2$ and *cis*-Rh(CO)(Cl)$(PR_3)_2$ are shown. For both *cis*- and *trans*-Rh(CO)(Cl)$(PR_3)_2$, the Rh−PR_3 bond energies increase with increasing σ-donor character of PR_3. The absolute bond energies are systematically smaller for the cis complex. Bond energies of both Rh−P bonds of *cis*-Rh(CO)(Cl)$(PR_3)_2$ (i.e., PR_3 trans to Cl and CO) have been examined and found to differ only by less than 0.5 kcal/mol. Taken together, all results indicate that *trans* influences do not dictate the opposing trends observed in Rh−PR_3 bond energies. Before turning our attention to the influence of effective charges on Rh−PR_3 bond energies, we make a brief diversion to examine the correlation of computed geometries with empirical data.

(B) Computed and Experimental Geometries. Interpretation of experimental data via comparison with computed data requires that computations adequately reproduce the experimental geometries. Table 3a shows the optimized geometries for the model complexes HPNPRh−PR_3, HP(CH)PRh−PR_3, and FPNPRh−PR_3 at B3LYP/LANL2DZ and BP86/TZ(P) levels of theory. For HPNPRh−PR_3 and HP(CH)PRh−PR_3 complexes, the results have been shown for both Me and H as substituents on the ligand PR_3. For FPNPRh−PR_3, where F is used as the substituent on the tridentate P, only Me is used on PR_3. BP86/TZP results are shown only for HPNPRh−PR_3 complexes. Experimental geometries for RPNPRhPPh_3 and RPNPRhP$(pyrl)_3$, also, are given. The calculated bond lengths are in good agreement with the experimental geometries, which justifies the use of model ligands in the computations.

Table 4. Natural Charge on the Elements for HPNPRh−PR_3, FPNPRh−PR_3, and Rh(CO)(Cl)$(PR_3)_2$ at the B3LYP/LANL2DZ Level of Theory

	PMe_3	PMe_2F	$PMeF_2$	PF_3
HPNPRh−PR_3/*FPNPRh−PR_3*				
Rh	−0.299	−0.296	−0.302	−0.307
	−0.372	*−0.367*	*−0.395*	*−0.409*
P(1)[a]	+1.000	+1.330	+1.609	+1.855
	+1.019	*+1.360*	*+1.655*	*+1.906*
N	−1.599	−1.594	−1.587	−1.576
	−1.599	*−1.594*	*−1.587*	*−1.570*
P(2)[b]	+0.482	+0.471	+0.499	+0.485
	+1.658	*+1.665*	*+1.683*	*+1.692*
Rh(CO)(Cl)$(PR_3)_2$				
Rh	−0.195	−0.237	−0.257	−0.282
P	+1.017	+1.370	+1.682	+1.947
Cl	−0.632	−0.587	−0.524	−0.461
C	+0.531	+0.548	+0.533	+0.546

[a] Phosphorus atom in PR_3 ligand. [b] Phosphorus atom in PNP fragment.

In Table 3b, B3LYP/LANL2DZ- and BP86/TZP-optimized bond lengths for the *trans*-Rh(CO)(Cl)$(PR_3)_2$ complexes are displayed. B3LYP/LANL2DZ-predicted results are shown for both Me and H in PR_3 as substituents along with F. The BP86/TZP results are only available for R = H, F.

The *trans*-Rh(CO)(Cl)$(PR_3)_2$ system shows the same trend as observed in the experiments. The Rh−PR_3 bond lengths become longer as increasingly σ-donating ligands are used on PR_3. The Rh−Cl bonds also become longer, but the Rh−CO bonds shorten, with increasingly σ-donating ligands. Consequently, the C−O bond length increases. Of course, these behaviors are consistent with the expectation that increasing the donor ability of PR_3 will enhance the Rh→CO π-back-donation.

(C) Effective Charges via NBO Analysis. Up to this point, it would appear that the trends in Rh−P bond energies can be traced to the amount of electron density centered on Rh: i.e., the charge. Table 4 shows the charge on the rhodium and coordinated atoms in HPNPRh−PR_3, FPNPRh−PR_3, and Rh(CO)(Cl)$(PH_3)_2$ complexes from the NBO analysis with R = Me.

The results show that the net charge on rhodium is negative and small and varies little with the nature of the ligand. The rhodium charge in HPNPRh−PR_3 is slightly more negative than in Rh(CO)(Cl)$(PH_3)_2$. These results demonstrate a surprising invariance of electron density at the Rh and demonstrate that Rh−P enthalpy trends are not rationalized by the simplistic notion of charge on the metal, at least as judged by the NBO analysis. In contrast to the Rh charges, the charges on

Table 5. Results of Charge Decomposition Analysis (CDA): Calculated (B3LYP/LANL2DZ) Donation *d*(A→B), Back-Donation *b*(B→A), Repulsive Polarization *r*(A↔B), and Residual Term (Δ) between the Ligand A and the Fragment B in the Complex C

complex	*d*(A→B)	*b*(B→A)	*b*/*d*	*r*(B↔A)	Δ
(a) $HPNPRhPR_3$					
$C = HPNPRhPH_3$, $A = PH_3$, $B = HPNPRh$	0.345	0.179	0.519	−0.343	0.004
$C = HPNPRhPH_2F$, $A = PH_2F$, $B = HPNPRh$	0.321	0.244	0.760	−0.327	0.004
$C = HPNPRhPHF_2$, $A = PHF_2$, $B = HPNPRh$	0.199	0.268	1.347	−0.320	0.001
$C = HPNPRhPF_3$, $A = PF_3$, $B = HPNPRh$	0.091	0.269	2.956	−0.328	0.004
(b) *trans*-$Rh(Cl)(CO)(PR_3)_2$					
$C = Rh(Cl)(CO)(PH_3)_2$, $A = PH_3$, $B = Rh(Cl)(CO)(PH_3)$	0.350	0.121	0.346	−0.274	−0.003
$C = Rh(Cl)(CO)(PH_2F)_2$, $A = PH_2F$, $B = Rh(Cl)(CO)(PH_2F)$	0.263	0.157	0.597	−0.257	−0.013
$C = Rh(Cl)(CO)(PHF_2)_2$, $A = PHF_2$, $B = Rh(Cl)(CO)(PHF_2)$	0.145	0.160	1.103	−0.279	−0.020
$C = Rh(Cl)(CO)(PF_3)_2$, $A = PF_3$, $B = Rh(Cl)(CO)(PF_3)$	−0.020	0.126	6.3	−0.276	−0.025
$C = Rh(Cl)(CO)(PH_3)_2$, $A = CO$, $B = Rh(Cl)(PH_3)_2$	0.474	0.360	0.759	−0.306	−0.009
$C = Rh(Cl)(CO)(PH_2F)_2$, $A = CO$, $B = Rh(Cl)(PH_2F)_2$	0.369	0.305	0.826	−0.310	−0.012
$C = Rh(Cl)(CO)(PHF_2)_2$, $A = CO$, $B = Rh(Cl)(PHF_2)_2$	0.330	0.300	0.909	−0.338	−0.017
$C = Rh(Cl)(CO)(PF_3)_2$, $A = CO$, $B = Rh(Cl)(PF_3)_2$	0.288	0.245	0.851	−0.356	−0.017
(c) $HP(CH)PRhPR_3$ and $FPNPRhPR_3$					
$C = HP(CH)PRhPH_3$, $A = PH_3$, $B = HP(CH)PRh$	0.263	0.146	0.555	−0.382	0.006
$C = HP(CH)PRhPH_2F$, $A = PH_2F$, $B = HP(CH)PRh$	0.241	0.213	0.883	−0.359	0.002
$C = HP(CH)PRhPHF_2$, $A = PHF_2$, $B = HP(CH)PRh$	0.122	0.244	2.000	−0.378	−0.002
$C = HP(CH)PRhPF_3$, $A = PF_3$, $B = HP(CH)PRh$	−0.070	0.245	3.500	−0.395	−0.002
$C = FPNPRhPMe_3$, $A = PMe_3$, $B = FPNPRh$	0.428	0.148	0.346	−0.025	−0.023
$C = FPNPRhPMe_2F$, $A = PMe_2F$, $B = FPNPRh$	0.282	0.182	0.645	−0.259	−0.029
$C = FPNPRhPMeF_2$, $A = PMeF_2$, $B = FPNPRh$	0.121	0.192	1.586	−0.250	−0.030
$C = FPNPRhPF_3$, $A = PF_3$, $B = FPNPRh$	−0.016	0.196	12.3	−0.252	−0.019

P of coordinated PR_3 are positive and change significantly from PMe_3 to PF_3. Nitrogen charge remains constant, as does the charge on carbon of CO. Phosphorus atoms in FPNP fragments are more positive than those in HPNP fragments, as expected; neither the FPNP P charges nor the HPNP P charges change as the PR_3 ligand is changed. The chlorine atom in $Rh(CO)(Cl)(PH_3)_2$ becomes less negative as PR_3 varies from PMe_3 to PF_3.

(D) Bonding Analysis. The electronic structures of complexes containing H and F as PR_3 substituents have been analyzed using charge decomposition analysis (CDA). The CDA clearly reveals the donor−acceptor nature of bonding in these complexes. We have performed CDA for the smaller system with hydrogen and fluorine as PR_3 substituents, except in $FPNPRh-PR_3$ complexes, where Me and F are used as PR_3 substituents. All CDA results indicate that it is appropriate to interpret the bonding in terms of the Dewar−Chatt−Duncanson model (as indicated by the very low residual terms in the CDA results[34]). Table 5a shows calculated $R_3P\rightarrow$RhHPNP σ-donation and $R_3P\leftarrow$RhHPNP π-back-donation for $HPNPRh-PR_3$ complexes. A plot of donation and back-donation is shown in Figure 4a. The table also shows the ratio of back-donation to donation (*b*/*d*) in both the complexes along with repulsive polarization *r* and residual terms Δ. Analogous data for the $Rh(CO)(Cl)(PR_3)_2$ series are provided in Table 5b and Figure 4b. Table 5c shows calculated $R_3P\rightarrow$RhFPNP, $R_3P\rightarrow$RhHP(CH)P σ-donation, and $R_3P\leftarrow$RhFPNP and $R_3P\leftarrow$RhHP(CH)P π-back-donation for $FPNPRh-PR_3$ and $HP(CH)PRh-PR_3$ complexes. Parts a and b of Figure 4 also show plots of donation and back-donation in $HP(CH)PRh-PR_3$ and $FPNPRh-PR_3$ complexes in comparison to $HPNPRh-PR_3$ and $Rh(CO)(Cl)(PR_3)_2$, respectively. In Figure 4c a plot of donation and back-donation through the Rh−CO bond in the $Rh(CO)(Cl)(PR_3)_2$ complexes is shown.

As expected, CDA demonstrates that $R_3P\rightarrow$Rh σ-donation decreases with increasingly π-accepting phosphines for $HPNPRh-PR_3$, $Rh(CO)(Cl)(PR_3)_2$, $FPNPRh-PR_3$, and $HP(CH)PRh-PR_3$ complexes. Two distinguishing features of $Rh(CO)(Cl)(PR_3)_2$ are that $R_3P\leftarrow$Rh π-back-donation is unchanged but OC←Rh π-back-donation decreases, from PH_3 to PF_3 (Figure 4b,c). One can view these effects as follows: binding of a donor ligand's lone pair to a coordinatively unsaturated metal complex necessarily increases the electron density at the metal. If the complex contains a strong π-accepting ligand such as CO, the increased density at the metal can be relieved by back-donation to CO. Thus, $Rh(CO)(Cl)PR_3-PR_3$ bond energies increase with greater PR_3 σ-donation because there is more net charge transfer from PR_3 to the metal and the Rh−CO bond is strengthened. Strong π-acceptor ligands effect little charge transfer from P to Rh and weaken the Rh−CO interaction by decreasing Rh→CO back-donation. A similar synergy is observed in the case of $FPNPRh-PR_3$ complexes (Figure 4b), where the fluorophosphines FPNP act as the π-acceptors. Overall, the charge on the metal changes little upon coordination, which is reminiscent of Pauling's electroneutrality principle.[35]

In contrast, the $HPNPRh-PR_3$ and $HP(CH)PRh-PR_3$ complexes lack a strong π-acceptor ligand. For these complexes, charge transfer from PR_3 to Rh cannot be accommodated. Instead, stabilization is gained via π-back-donation from Rh to PR_3, which strengthens the Rh−N and Rh−C σ bonds. Thus, the $HPNPRh-PR_3$ and $HP(CH)PRh-PR_3$ bond enthalpies increase with increased electronegativity of the PR_3 substituent.

(34) (a) Frenking, G.; Pidun, U. *J. Chem. Soc., Dalton Trans.* **1997**, 1653−1662. (b) Dapprich, S.; Frenking, G. *Angew. Chem.* **1995**, *107*, 383−386; *Angew. Chem., Int. Ed. Engl.* **1995**, *34*, 354−357. (c) Ehlers, A. W.; Dapprich, S.; Vyboishchikov, S. F.; Frenking, G. *Organometallics* **1996**, *15*, 105−117. (d) Dapprich, S.; Frenking, G. *Organometallics* **1996**, *15*, 4547−4551. (e) Pidun, U.; Frenking, G. *J. Organomet. Chem.* **1996**, *525*, 269−278. (f) Weiss, J.; Stetzkamp, D.; Nuber, B.; Fischer, R. A.; Böhme, C.; Frenking, G. *Angew. Chem.* **1997**, *109*, 95−97; *Angew. Chem., Int. Ed. Engl.* **1997**, *35*, 70−72.

(35) Pauling, L. *J. Chem. Soc.* **1948**, 1461.

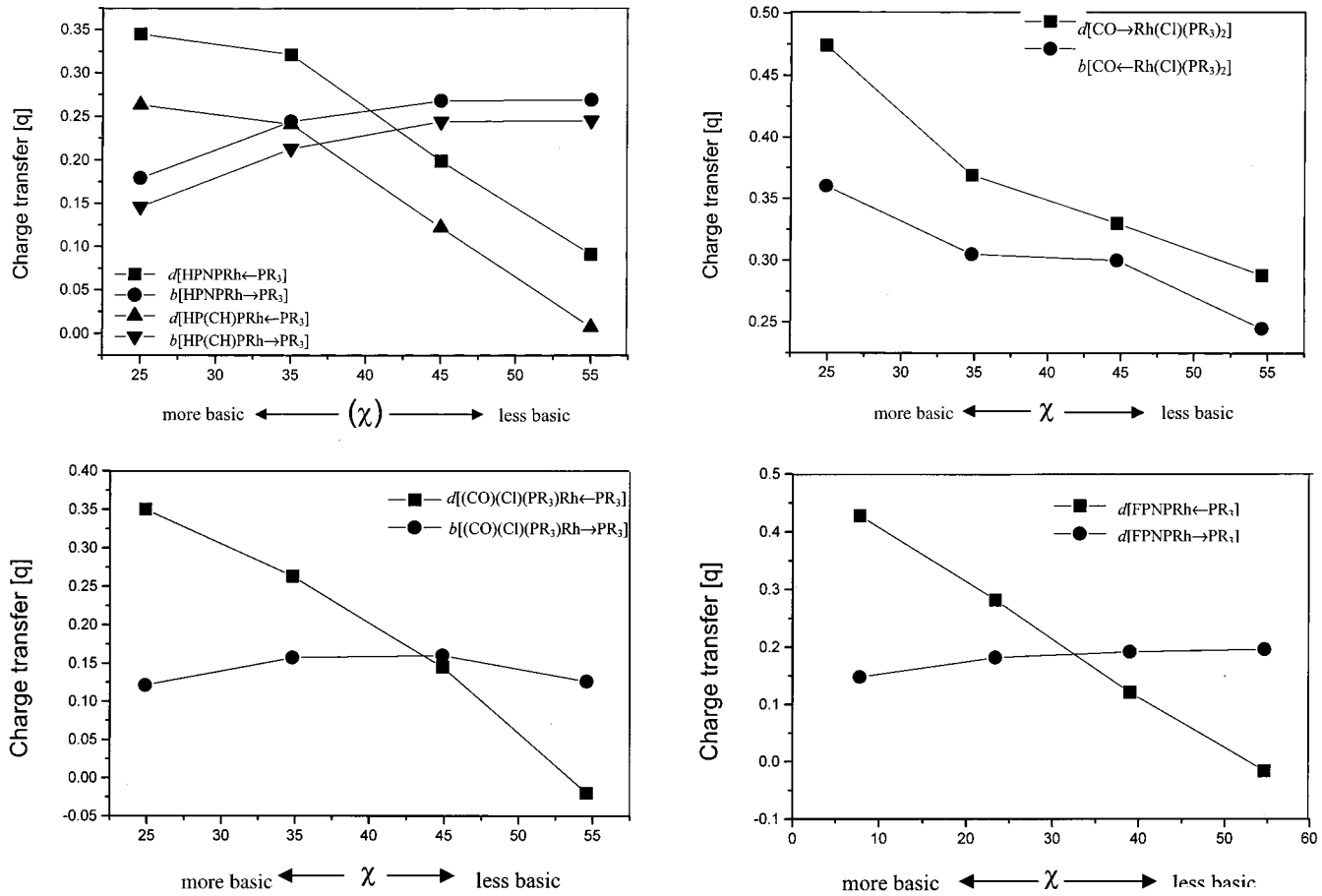

Figure 4. Rh←PR_3 charge donation *d* and Rh → PR_3 charge back-donation *b*, calculated at the B3LYP/LANL2DZ level, for model complexes plotted against Tolman χ parameters for the ligands PR_3: (a, top left) HPNPRh−PR_3 and HP(CH)-PRh−PR_3; (b, bottom two) Rh(CO)(Cl)$(PR_3)_2$ and FPNPRh−PR_3; (c, top right) Rh(Cl)$(PR_3)_2$−CO.

4. Discussion

Our work shows that computations reproduce the opposing trends seen for the enthalpies of reactions 1 and 2 as a function of the PR_3 Tolman electronic parameter. The novel finding is that the reorganization energies RE(Rh−P) in both reactions are very small and relatively constant. Thus, *the contradictory trends are not due to reorganization energies*. It follows that the origin of the contradictory trends resides in the fundamental bonding of the HPNPRh−PR_3 and Rh(CO)(Cl)-$(PR_3)_2$ molecules.

Another important result is that the BE(Rh−P) enthalpy trends in HPNPRh−PR_3, FPNPRh−PR_3, HP-(CH)PRh−PR_3, and Rh(CO)(Cl)$(PR_3)_2$ complexes confirm that *Rh−P bond strengths are not universal and not transferable*. The calculations also show that moving of the PR_3 ligand from the trans position to a cis position does not alter the bond enthalpy trend. Use of non-π-donating ligands such as HP(CH)PRh−PR_3 does not change the observed order of Rh−PR_3 bond energies from that seen in π-donating HPNPRh−PR_3, although it does systematically weaken the Rh−PR_3 bonds by 7−10 kcal/mol. Presumably, bond weakening is seen because N→Rh π-donation enhances Rh → PR_3 π-back-donation. The bond enthalpy trend seen for HPNPRh−PR_3 can be reversed by making the PNP ligand a good π-acceptor (FPNPRh−PR_3).

The optimized geometries for the model complexes are in satisfactory agreement with the comparable experimental geometries. BP86/TZP calculations, which use Slater-type orbitals, reproduce bond lengths at Rh better than B3LYP/LANL2DZ. The calculations show that the Rh−PR_3 bond lengths shortened with increasing number of π-accepting F-substituted phosphines in all complexes; hence, bond lengths and bond energies are not correlated. Increasing the electronegativity of the PR_3 substituent contracts the phosphorus orbitals, leading to shorter Rh−P bonds. Rh−CO bond lengths increase with increasingly π-accepting PR_3, due to lowered π-back-donation.

Rhodium remains a 16e center in the complexes with a slightly negative charge on Rh, regardless of PR_3. Synergistic $\sigma-\pi$ type donor−acceptor interactions provide a simple model to explain the bond enthalpy trend in these complexes. If a good π-acceptor ligand is present (such as CO), Rh−P bond strengths increase with phosphorus σ-donor strength. If there is not a good π-acceptor ligand, the Rh−P bond strengths increase with π-accepting capacity of phosphorus. Our computations indicate that rhodium acts as a domain of fixed electrons with slightly negative charge. Pauling's electroneutrality principle[35] is fairly applicable in these rhodium complexes. Electron push and pull through $\sigma-\pi$ is the most important way of describing the bonding nature in the complexes without a change of the effective charge on rhodium. Although these synergistic $\sigma-\pi$ interactions provide a useful model *ex post*

facto, the net balance of these interactions is subtle and difficult to predict a priori.

5. Conclusion

The concerns which have been posed at the end of the introduction can now be addressed as follows.

(1) Reorganization energies are unimportant in the contradictory reaction enthalpy trends in Rh(I)−phosphine systems.

(2) The synergistic σ and π donor−acceptor interactions are critical in determining the bond enthalpy trends of reactions 1 and 2.

(3) The computations also confirm that the Rh−P bond strengths are nontransferable from one system to another because the Rh−P bond strength is largely determined by the relative importance of Rh←PR_3 (σ) and Rh→PR_3 (π) bonding, which varies with the nature of the other ligands attached to Rh.

Acknowledgment. This work was supported by the National Science Foundation (Grant No. CHE-9618497) and through a DuPont Grant-In-Aid.

OM000544+